Developmental Biology 433 (2018) 61–74

Contents lists available at ScienceDirect

Developmental Biology

journal homepage: www.elsevier.com/locate/developmentalbiology

Original research article

Nasal and otic placode specific regulation of *Sox2* involves both activation by Sox-Sall4 synergism and multiple repression mechanisms

Satoko Sugahara[a], Tooru Fujimoto[a], Hisato Kondoh[b,*], Masanori Uchikawa[a,*]

[a] Graduate School of Frontier Biosciences, Osaka University, 1-3 Yamadaoka, Suita, Osaka 565-0871, Japan
[b] Faculty of Life Sciences, Kyoto Sangyo University, Motoyama, Kamigamo, Kita-ku, Kyoto 603-8555, Japan

ARTICLE INFO

Keywords:
Sensory development
Nasal and otic placodes
Sox2 NOP1 enhancer
Sall4
Sox factors
Zeb and Snail factors

ABSTRACT

Transcription factor gene *Sox2* is expressed throughout sensory development, but the enhancers that regulate the gene vary depending on the developmental stages and tissues. To gain new insights into the gene regulatory network in sensory placode specification, regulation of the nasal-otic bispecific NOP1 enhancer of *Sox2* was investigated in chicken embryos. Deletion and mutational analyses using electroporation showed that transcriptional repression mechanisms in combination with activation mechanisms determine placodal specificity. Activation of the NOP1 enhancer involves synergistic action by Sall4 and SoxB1/SoxE factors that bind to the adjacent sites. Deletion of repressive elements resulted in widening of the tissue area for enhancer activity to a region where the expression of *Sall4* and *SoxB1/E* overlaps, e.g., the CNS and neural crest. Among multiple repressive elements that contribute to the placodal confinement of the NOP1 enhancer activity, CACCT/CACCTG motifs bound by Zeb/Snail family repressors play important roles. Overexpression of δEF1 (Zeb1) or Snail2 (Slug) strongly inhibited NOP1 activity. These data indicate that both activation by Sall4-Sox synergism and multiple repression mechanisms involving Zeb/Snail factors are essential for *Sox2* regulation to be confined to the nasal and otic placodes.

1. Introduction

Sensory organ primordia are derived from the preplacodal region (PPR) of the cephalic ectoderm, and specified through multiple steps (Baker and Bronner-Fraser, 2001; Jacobson, 1963; Schlosser, 2006; Streit, 2004, 2007). The transcription factor (TF) gene *Sox2* is activated when the sensory primordia are formed in the PPR, and its expression is augmented when the sensory placodes are formed (Kamachi et al., 1998). Sox2 directly regulates the genes that are involved in the development of sensory primordia, such as the placode-characteristic cell adhesion molecules, N-cadherin and N-CAM (Matsumata et al., 2005), and the TF genes that operate during inner ear development (Ahmed et al., 2012; Evsen et al., 2013; Neves et al., 2012; Zou et al., 2008).

Although *Sox2* is commonly expressed in sensory primordia as well as in neural primordia at different developmental stages, it is regulated in a stage- and region-specific fashion by distinct enhancers (Kamachi et al., 2009; Okamoto et al., 2015; Uchikawa et al., 2003, 2004; Uchikawa and Kondoh, 2016). Many of these enhancers are scattered across a ~ 200 kb genomic region encompassing the *Sox2* gene, and are conserved across vertebrate species. This indicates that the mechanisms that activate *Sox2* in each subdomain of the sensory and neural primordia are common to vertebrate species.

The initial low-level *Sox2* expression in the cephalic ectoderm is regulated by the N4 enhancer (Saigou et al., 2010; Uchikawa et al., 2003; Uchikawa and Kondoh, 2016). The NOP1 and NOP2 enhancers are then activated in both the nasal and otic placodes, differentiating them from the lens placode represented by N3 enhancer activity (Inoue et al., 2007; Uchikawa et al., 2003). *Sox2* enhancers that are active in either the nasal or otic placodes are subsequently activated (Okamoto et al., 2015). These observations suggest that *Sox2* activation in the nasal and otic placodes initially depends on an analogous regulation, and then on each placode-specific regulation, possibly in response to local signaling cues.

To elucidate how *Sox2* activation in nasal and otic placode precursors is commonly regulated, we investigated the NOP1 enhancer with respect to the regulatory elements involved. An important finding was that the NOP1 enhancer is activated by the synergistic action of SoxB1/E TFs and Sall4, and superimposition of the effects of repressive elements delimits the activity of the enhancer to the nasal and otic placodes. Candidate repressor TFs that bind to the repressive elements of NOP1 and are expressed in the CNS and neural crest of the chicken

* Corresponding authors.
E-mail addresses: kondohh@cc.kyoto-su.ac.jp (H. Kondoh), uchikawa@fbs.osaka-u.ac.jp (M. Uchikawa).

https://doi.org/10.1016/j.ydbio.2017.11.005
Received 23 September 2016; Received in revised form 2 November 2017; Accepted 10 November 2017
Available online 11 November 2017

embryo include δEF1 (Zeb1), Sip1 (Zeb2) and Snail2 (Slug) (Del Barrio and Nieto, 2004; Funahashi et al., 1993; Jolma et al., 2013; Sekido et al., 1997; Verschueren et al., 1999; Yasumi et al., 2016).

2. Materials and methods

2.1. Construction of enhancer reporter plasmids, chicken embryo electroporation and embryonic culture

The NOP1 enhancer sequence and deletion/mutation variants of this sequence were inserted at the *Sma*I site of tk-EGFP or tk-mRFP1 vectors and subsequently dimerized using flanking restriction sequences with shared 4-base overhangs, as described by Kondoh and Uchikawa (2008) and Uchikawa et al. (2017). Multimerization of an enhancer sequence augments its activity and facilitates the detection of changes in this activity. Stage 4 chicken embryos were electroporated on the epiblastic side using a ~ 1 μl solution containing 3–4 μg of vector DNA, including 2 μg/μl of deleted or mutated versions of dimeric NOP1-tkEGFP and 1 μg/μl of wild-type dimeric NOP1-tkmRFP1, to evaluate the effects of deletions and mutations on the NOP1 enhancer. Electroporation was carried out with five electric pulses at 10 V per 4 mm inter-electrode distance, with 50 msec duration and 100 ms intervals (Hatakeyama and Shimamura, 2008; Uchikawa, 2008; Uchikawa et al., 2003). Electroporated embryos were cultured using a modified New's technique as described by Uchikawa et al. (2003), and staged according to Hamburger and Hamilton (1951). Fluorescence signals were photo-recorded at intervals. The relative fluorescence intensities of EGFP representing enhancer activity of test sequences compared with control (wild type) enhancer-dependent mRFP1 fluorescence were used to assess the effects of the deletions or mutations.

2.2. Vectors of exogenous genes

To express exogenous genes in the posterior cephalic ectoderm of chicken embryo by electroporation, the octamerized N4 enhancer HE fragment carrying an ectoderm-specific element, N4HEx8 (Saigou et al., 2010), was used. cDNAs for C-truncated Sox2 proteins were fused to an engrailed repression domain sequence to produce Sox2(183)EnR or Sox2(120)EnR and were used to replace the EGFP sequence of N4HEx8-tkEGFP. An H4HEx8 sequence was also inserted at the *Sma*I site of ptkmRFP1ver2 (Kondoh and Uchikawa, 2008; Uchikawa et al., 2017) to produce the N4HEx8-tkmRFP1 reporter which shows regional coverage of the N4HEx8 enhancer. The DNA solution containing 2 μg/μl of wild-type dimeric NOP1-tkEGFP, 2 μg/μl of N4HEx8-vector, and 0.5 μg/μl of N4HEx8-tkmRFP1 was used. To overexpress δEF1 or Snail2, full-length chicken cDNA sequences were inserted in the above-mentioned N4HEx8-vector and pCAGGS vector (Niwa et al., 1991). When the pCAGGS vector was used, the NOP1-tkEGFP vector (2 μg/μl) was electroporated in embryos at st. 4 and then pCAGGS-δEF1/Snail2 (1 μg/μl) was electroporated on one side of embryos with pCMV-mRFP1 (0.1 μg/μl) at st. 7 to examine the effect of δEF1/Snail2 on NOP1 enhancer activity.

2.3. Sequence analysis

DNA sequences were analyzed using the MacVector software (MacVector, Inc.). To compare the DNA sequences, Pustell matrix analysis was performed using window size of 12, minimum score of 60, and hash value of 6. Putative binding sequences of TFs were assigned using the following consensus sequences: δEF1/Sip1 CACCT (Sekido et al., 1997; Verschueren et al., 1999), Snail2 and E2 box CACCTG (Batlle et al., 2000; Cano et al., 2000), Fgf-response element TGTGAC (Takemoto et al., 2006) allowing a single base mismatch, Fox factors T[A/G]TTT[A/G][C/T] (Overdier et al., 1997), GATA factors [A/T]GATA[A/G] (Ko and Engel, 1993), homeodomain (HD) factors ATTA (Jolma et al., 2013), Lef/Tcf factors [T/A][T/A]CAAA(G) (Giese et al., 1991), Sox factors [A/T][A/T]CAA[A/T](G) (Kamachi and Kondoh, 2013), Six factors TCAGGTT (Spitz et al., 1998) allowing 2 mismatches, and Sall4 [C/T]AGAGC (Cho et al., 2008).

2.4. Whole mount in situ hybridization

Whole mount in situ hybridization was performed as described previously (Uchikawa et al., 2003) using probes for *Sox2* (462–1013 of GenBank ID: D50603), *Sox3* (676–1382 of GenBank ID: AB011803), *Sox8* (935–1523 of GenBank ID: AF228664), *Sox9* (740–1348 of GenBank ID: AB012236), and *Sall4* (174–873 of GenBank ID: AY342354).

2.5. Luciferase assays

Primary fibroblasts were isolated from E14 chicken embryos using 0.1% collagenase and 0.025% trypsin and cultured in Dulbecco's modified Eagle's MEM (DMEM) containing 10% fetal calf serum (FCS). After two days, the cells were dissociated using 0.025% trypsin and 0.24 mM EDTA, and replated in Ham's F12 medium with 10% FCS in 24-well plates at the cell density of 4×10^4 per well for transfection on the following day. Cells in each well were transfected with 0.2 μg DNA using Fugene 6 reagent (Roche). The DNA contained 80 ng of expression vectors for *Sall4*, *SoxB1/E* and/or an empty vector, 100 ng of firefly luciferase reporter vector carrying an octamerized NOP1 core sequence, and 20 ng of Renilla luciferase vector as a transfection control. Luciferase activities were measured at 48 h after transfection using the Dual Luciferase Assay System (Promega). Data from multiple transfections were averaged and are shown with standard errors.

2.6. Chromatin immunoprecipitation-quantitative polymerase chain reaction (ChIP-qPCR) analysis

Head tissues of stage 11–12 embryos anterior to the fourth somite level were dissected in cold PBS supplemented with Protease Inhibitor Cocktail (#03969-21, Nacalai Tesque), homogenized, and fixed with 1% formaldehyde for 5 min, followed by addition of 125 mM glycine. The fixed tissues were further processed using the Chromatin Immunoprecipitation Assay Kit (#17-295, Upstate (Merck)) supplemented with the Protease Inhibitor Cocktail. Briefly, the tissues were washed with cold PBS, resuspended in SDS lysis buffer, and treated with an S220 Focused-ultrasonicator (Covaris) to fragment chromatin DNA to an average size of 500 bp. The sonicates were diluted 10-fold in ChIP dilution buffer to quench the SDS, and incubated overnight with the anti-Sall4 rabbit antibody (ab29112, Abcam) or normal rabbit IgG (#2729, Cell Signaling Technology). The chromatin-antibody complexes were isolated using protein A agarose, washed, eluted using the elution buffer, and released from cross-linking by incubation at 65 °C overnight in 0.2 M NaCl. After RNase A and proteinase K treatments, DNA fragments were purified using the Zymo-Spin™ ChIP kit (Zymo Research) and analyzed using the SYBR Green qPCR kit (RR820, Takara) in a StepOnePlus Real-Time PCR System (Applied Biosystems). Sall4 binding in the following genomic regions were assessed by qPCR: Sall4-Sox binding regions of NOP1 and NOP2, a region of the chromosome 4 gene desert (the control region used by Murko and Bronner (2017)), and ovalbumin intron 1. The following primer pairs were used: NOP1_F 5′-AAAGGTGTTGAGGGCAGGTC-3′ and NOP1_R 5′-CCGTGGTGCTTTTGATCAGC-3′; NOP2_F 5′-GCAA CACCGCTTAACTGCAT-3′ and NOP2_R 5′-GCTAACTAGCGGGCGA TCAA-3′; Chr4_F 5′-GGTTGGATTTCCAGTCTCCA-3′ and Chr4_R 5′-TGTTTTGCTGGACAATCTGC-3′ (Murko and Bronner, 2017); ovalbumin_F 5′-ACTGCATAGCTCAGAGGCTG-3′ and ovalbumin_R 5′-ACACTCTGGGAGTTGGAGGT-3′, which produced PCR products of 107 bp, 169 bp, 69 bp, and 75 bp, respectively.

3. Results

3.1. Characterization of the NOP1 enhancer

NOP1 enhancer activity was investigated following developmental stages after electroporation of stage (st.) 4 chicken embryo with NOP1×2-tkEGFP (Fig. 1A). The enhancer was initially activated in the nasal placode-forming ectoderm at st. 9, and then in the otic placode at st. 10. Strong NOP1 activity was established at around st. 10–11 when these placodes are fully specified and can carry out autonomous development in ectopic embryonic sites (Bhattacharyya and Bronner-Fraser, 2008; Groves and Bronner-Fraser, 2000). In the otic placode, the NOP1 activity was prominent in the caudal portion. Low enhancer activity in the caudal spinal cord was also detectable. The NOP1 activity in the nasal and otic placodes persisted up to st. 16 of embryogenesis, the limit of the electroporated chicken embryo culture. Previously reported electroporation experiments using otocyst electroporation have indicated that NOP1 activity persists until later sensory patches (Evsen et al., 2013; Neves et al., 2011, 2012).

The NOP1 enhancer sequence is strongly conserved in various vertebrate species other than fish (Uchikawa, 2008), as shown by our alignment of the NOP1 sequences of chicken, human, mouse and *Xenopus* (Fig. 1B). Many sequence motifs for potential TF binding sites in the NOP1 enhancer 1-15) were recognized as shown in Fig. 1B.

A comparison of the NOP1 sequence with that of NOP2, a second enhancer with similar nasal and otic placode specificity, indicated an interesting commonality. Whilst no extensive similarities exist between the NOP1 and NOP2 sequences, Pustell DNA matrix analysis revealed a few stretches of sequences conserved between NOP1 and NOP2 (Fig. 1C), which include the set of sequence motifs CTTTGT (Motif 8) and [C/T]AGAGC (Motif 7) (Fig. 1B). Given that CTTTGT is a canonical Sox binding sequence and that Sox proteins often cooperate with a partner factor that binds to a neighboring DNA site (Kamachi et al., 2000; Kondoh and Kamachi, 2010), we speculated that the [C/T] AGAGC (Motif 7) sequence is the binding site for a partner factor.

3.2. Deletion analysis of the NOP1 enhancer showing involvement of both activating and repressive elements

We investigated the regulatory elements involved in NOP1 enhancer activity, via stepwise deletions from either end of the 334-bp NOP1 sequence (Fig. 2Aa). The enhancer activity of the deleted versions of NOP1 was compared with that of the full-length NOP1 in co-electroporated chicken embryos (Fig. 2B and Table 1).

The del-1 mutant lacking the 5′ 20 bp showed significantly reduced NOP1 enhancer activity, and del-3 with a further deletion to 60 bp inactivated the enhancer activity in the otic placode, while some activity was still observed in the nasal placode (Suppl. Fig. 1A). A deletion of 109 bp from the 5′ side (del-6) totally inactivated the NOP1 enhancer. These results suggest that the 5′ half of the NOP1 sequence contains several activation elements.

By contrast, deletions from the 3′ end of NOP1 augmented the enhancer strength in a stepwise manner and widened its region of activity in non-placodal tissues (Fig. 2B, Suppl. Fig. 1A, and Table 1). Deletion from the 3′ end to 271 bp (del-8) augmented the enhancer activity in the nasal and otic placodes, and expanded the enhancer-active areas in the cephalic ectoderm. Deletion to 214 (del-9) caused additional activation of the enhancer in the brain, and a further deletion to 194 (del-10) increased the enhancer activity in the brain and extended this activity to the entire spinal cord. Deletion to 174 (del-11) strongly enhanced the NOP1 enhancer activity with expansion to the cephalic neural crest and mesenchymal cells underlying the cephalic ectoderm. These results suggest that the 3′ half of the NOP1 sequence contains several repressive elements, which together delimit the enhancer activity to the nasal and otic placodes.

A further 20 bp deletion from the 3′ side to 154 bp (del-12) markedly reduced NOP1 enhancer activity which remained in the nasal and otic placodes only, thus eliminating all of the non-placodal enhancer activity observed for del-11. This indicated that the region from 154 to 173 bp contains an element that strongly augments NOP1 enhancer activity. Extension of the deletion to 134 did not affect this activity any further, but progression of deletion from 134 bp to 110 bp (del-14) completely inactivated the enhancer activity, indicating that the 110–133 region, which includes sequence motifs 7 and 8, is essential for the activation of NOP1 in the nasal and otic placodes.

3.3. Mutational analysis identifying potential regulatory elements in the NOP1 sequence, highlighting Sox and partner TF binding elements

To evaluate the significance of sequence motifs for potential TF binding sites within the NOP1 enhancer, mutations were introduced into these fifteen sequence motifs (1–15) as shown in Figs. 1B and 2Ab. These mutational effects were then compared with the effects of the deletions described above (Fig. 2C, Suppl. Fig. 1B, and Table 2).

Mutations of either the motif 7 (TAGAGC) or motif 8 (Sox binding sequence CTTTGTT) significantly reduced enhancer activity, leaving only marginal activity in the nasal placode. This observation indicated that this motif pair, which is shared with NOP2, has a critical role in the regulation of NOP1 enhancer activity. Given that Sox class TFs in many cases functions in cooperation with a partner factor that binds to a nearby DNA site (Kamachi and Kondoh, 2013; Kamachi et al., 2000; Kondoh and Kamachi, 2010), the TAGAGC motif likely serves as this partner factor site.

Mutations in motifs 1, 4, 10, 11, 12, and 14 also caused a reduction in NOP1 enhancer activity, suggesting that these elements are involved in boosting the enhancer activity generated via motifs 7 and 8.

Mutations in motifs 2, 6, 9 and 15 augmented NOP1 enhancer activity in the nasal and otic placodes. Mutations also provoked ectopic enhancer activity in the forebrain and midbrain (motifs 9 and 15), and the midbrain-hindbrain boundary region (motif 6). These elements thus represent repressive elements.

These mutational analyses confirmed that multiple activating elements contribute to the nasal and otic placode-specific activity of NOP1, and also that repressive elements play crucial roles in restricting the enhancer activity of NOP1 to the nasal and otic placodes. Of these elements, motifs 7 and 8, which are involved in NOP1 activation, and motif 15, involved in enhancer repression, were investigated further.

3.4. NOP1 110–133 enhancer depends on TAGAGC and Sox binding sequences and is active broadly in neural, neural crest and placode cells

The results of our deletion and mutational analyses suggested an essential function of the Sox binding sequence of motif 8 and the putative partner TF binding sequence of motif 7 in the activation of the NOP1 enhancer in the nasal and otic placodes. To further analyze the mechanism of enhancer activation through these motifs, the isolated 110–133 bp region, containing motifs 7 and 8, was examined using the multimeric form (Fig. 3A). This strategy was taken because enhancer activity associated with regulatory element can be magnified by tandem multiplication of the sequence, particularly when the activity of the element in isolation is minute (Goto et al., 1990; Inoue et al., 2007; Kamachi and Kondoh, 1993; Kondoh and Uchikawa, 2008; Tanaka et al., 2004; Uchikawa et al., 2017).

An octamer of the 110–133 bp sequence showed strong enhancer activity in the nasal and otic placodes, the entire CNS, and the neural crest (Fig. 3B, C). The enhancer activity in the CNS was observed as early as st. 5, shortly after embryo electroporation, and persisted to later stages of neural development (st. 11). The transcriptional activation mediated by the 110–133 bp sequence is therefore not specific to the nasal and otic placodes. It is interesting to note that the enhancer activity of the 110–133 region octamer was almost identical to that of

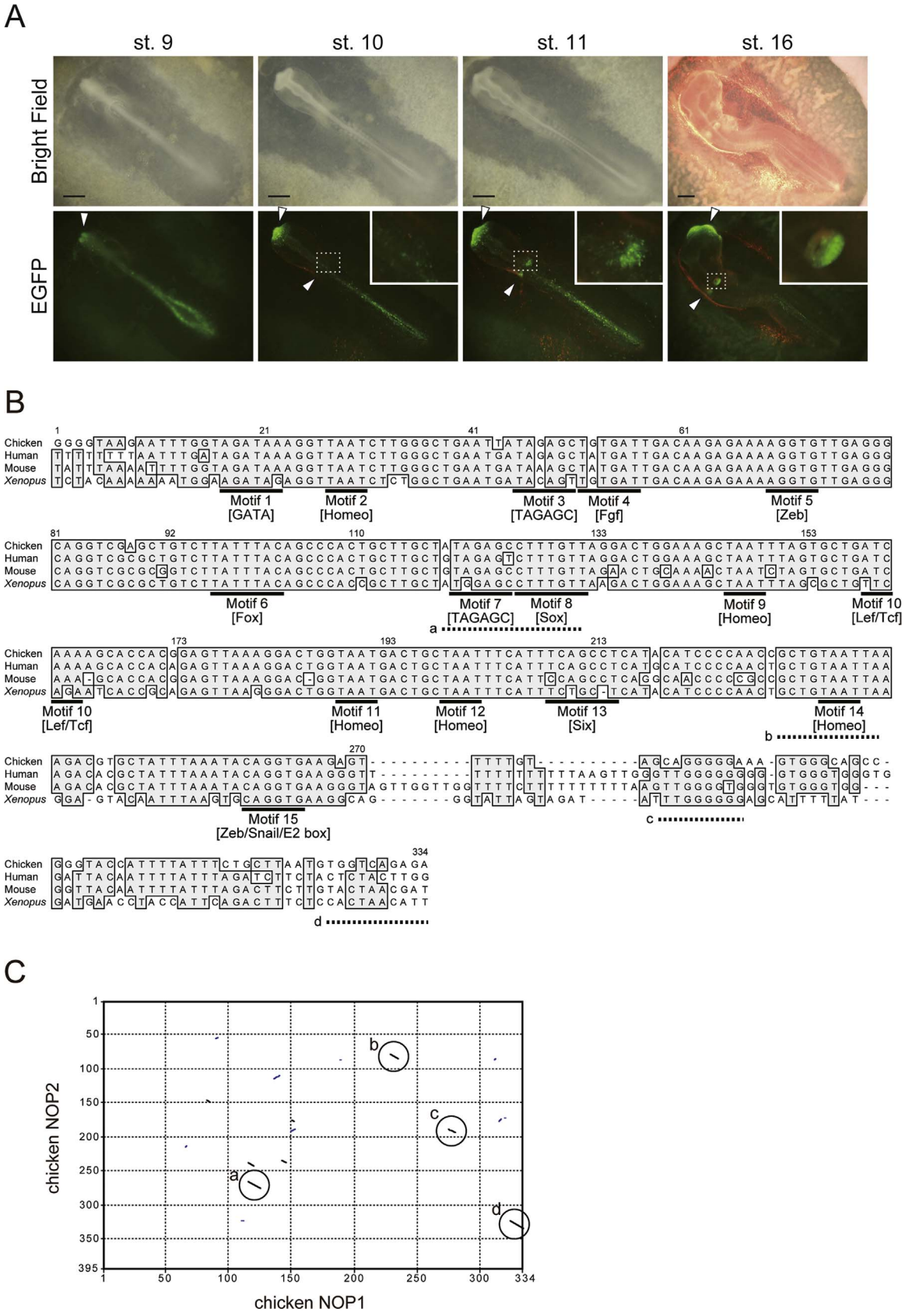

Fig. 1. Characterization of the NOP1 enhancer. (A) Time course activation profile of the NOP1 enhancer in an electroporated chicken embryo. NOP1 enhancer activity becomes detectable in the nasal placode region at st. 9 and in the otic placode region at st. 10. These activities are maintained up to st. 16. The red signal is a spillover of strong red fluorescence from the CMV-mRFP1 vector which was coelectroporated. Concerning the st. 16 specimen, the mRFP1 fluorescence image was superimposed on the brightfield-image to demonstrate successful electroporation in a wide embryonic area. Scale bars, 500 μm. (B) Alignment of the chicken NOP1 sequence with that of human, mouse and *Xenopus*. Sequence motifs 1–15 are indicated. Number of chicken NOP1 sequence is annotated above sequence. Dotted lines indicate the sequences conserved between the NOP1 and NOP2 enhancers as determined in (C). (C) Comparison of the NOP1 and NOP2 enhancer sequences from the chicken using a Pustell dot matrix. The regions of sequence similarity are encircled.

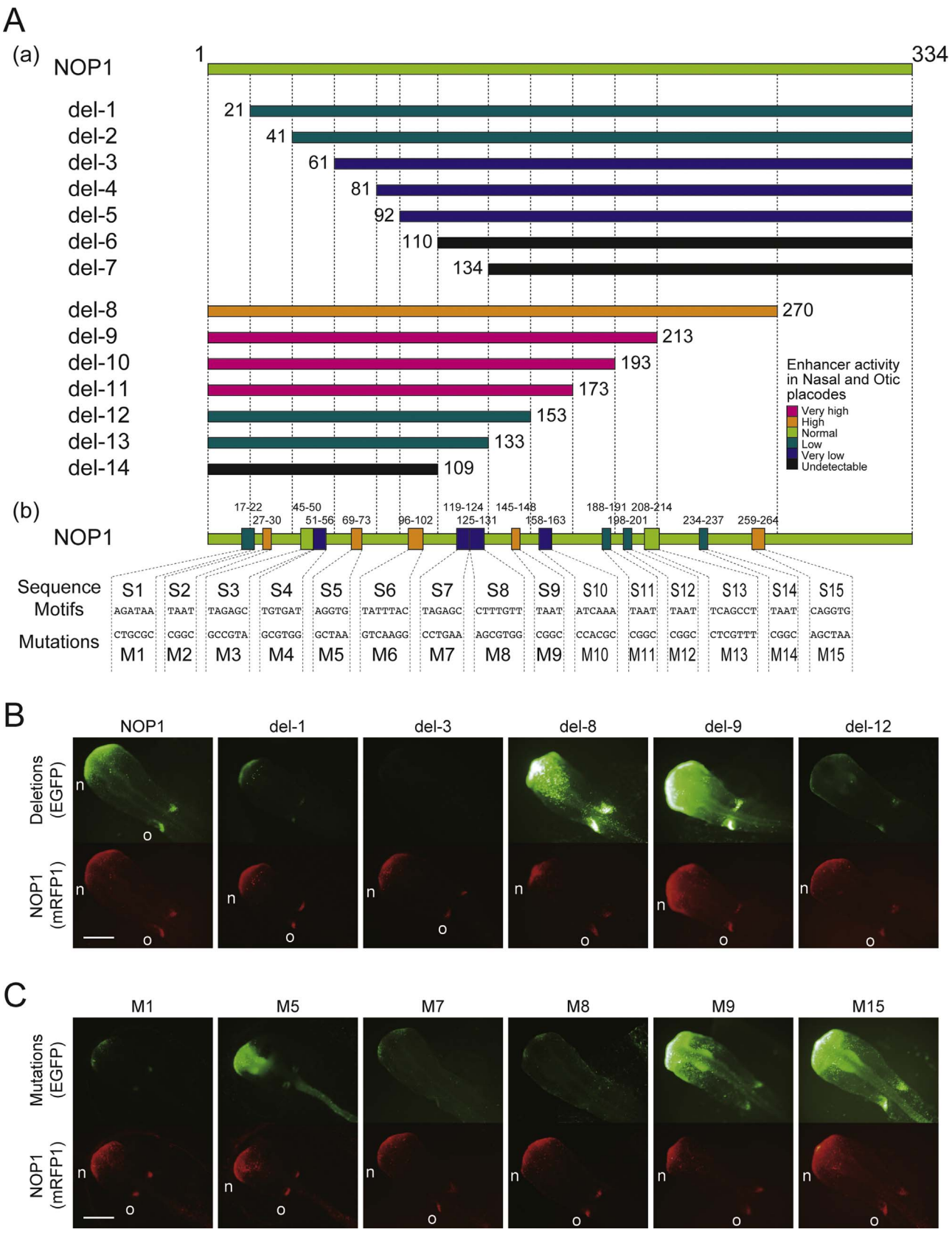

Fig. 2. Deletion and mutational analyses of the regulatory elements of NOP1. (A) Schematic representation of the NOP1 sequence and its subfragments and their enhancer activities in the nasal and otic placodes. (a) Deletion mutant series starting from the 5′ or 3′ terminus of the NOP1 sequence and summary of their activities in electroporated embryos. (b) Schematic representation of sequence motifs 1-15) and introduced mutations (M1 to M15) in the NOP1 sequence and a summary of their effects. (B) Activities of representative deletion mutants of the NOP1 enhancer described in (A) in activating EGFP reporter in comparison with the activation of mRFP1 by full-length NOP1 in the same electroporated embryo. (C) Activities of the representative base-substitution mutants of the NOP1 enhancer described in (A) shown by EGFP activation in comparison with wild-type NOP1 activation of mRFP1. Nasal and otic placodes are denoted by “n” and “o”, respectively. Images of EGFP and mRFP1 signals in an embryo specimen were taken using the same capture period to compare the relative enhancer strengths. Data of mutants not shown in these panels are presented in Supplementary Fig. 1. Scale bars in (B) and (C), 500 μm.

Table 1
Effect of deletions from either side of the NOP1 sequence.

NOP1 deletions	Remaining sequences	Enhancer activity[a]			Number of specimens
		Nasal placode	Otic placode	CNS	
Full length	1–334	++	++	–	19
del-1	21–334	+	+	–	5
del-2	41–334	+	+	–	6
del-3	61–334	+/–	–	–	6
del-4	81–334	+/–	+/–[b]	+/–; fb, sc	5
del-5	92–334	+/–	–	+/–; fb, sc	5
del-6	110–334	–	–	–	2
del-7	134–334	–	–	–	3
del-8	1–270	+++	+++	–	9
del-9	1–213	++++	+++	+++; fb, mb	5
del-10	1–193	++++	++++	++++; fb mb, sc	5
del-11	1–173	++++	++++	+++++; CNS, nc	11
del-12	1–153	+	+	+; di, mb	5
del-13	1–133	+	+	+; di, mb	6
del-14	1–109	–	+/–[c]	–	6

CNS domains: fb, forebrain; di, diencephalon; mb, midbrain; sc, spinal cord; nc, neural crest.
[a] The relative enhancer strength: –, undetectable; +/–, very low activity detectable only after a long exposure; +, activity lower than normal; ++, activity comparable to wild type; +++, high activity; ++++ and +++++, very high activities.
[b] The activity was uniform in the entire otic placode tissue.
[c] The activity was not specific to the otic placode but broad in the cephalic ectoderm around the otic placode.

Table 2
Activities of the NOP1 mutants tested in this study.

NOP1 mutants	Characteristic of sequence motif	Position	Enhancer activity[a]			Number of specimens
			Nasal placode	Otic placode	CNS	
Wild type			++	++	–	19
M1	GATA	17–22	+	+	–	2
M2	Homeo	27–30	+++	+++	–	8
M3	[TAGAGC]	45–50	++	++	–	5
M4	Fgf	51–56	+/–	–	–	5
M5	Zeb	69–73	++	+[b]	+++; fb, sc	6
M6	Fox	96–102	+++	+++	+++; mb, mhb	6
M7	[TAGAGC]	119–124	+/–	–	–	7
M8	Sox	125–131	+/–	–	–	6
M9	Homeo	145–148	+++	++	+++; fb, mb	6
M10	Lef/Tcf	158–163	+/–	–	–	5
M11	Homeo	188–191	+	+	+/–; fb, mb	3
M12	Homeo	198–201	+	++[c]	+/–; fb, mb	3
M13	Six	208–214	++	++	–	5
M14	Homeo	234–237	+	+	–	2
M15	Zeb and Snail /E2 box	259–264	+++	+++	+++; fb, mb	8

CNS domains: fb, forebrain; mb, midbrain; mhb, midbrain-hindbrain boundary; sc, spinal cord.
[a] The relative enhancer strength: –, undetectable; +/–, very low activity detectable only after a long exposure; +, activity lower than normal; ++, activity comparable to wild type; +++, high activity.
[b] The activity was uniform in the entire otic placode tissue.
[c] The activity was stronger in the dorsal and posterior parts of the otic placode.

NOP1 del-11 in which the major repressing elements are deleted (Suppl. Fig. 1A). These observations indicated that the 110–133 bp sequence plays a central role in the activation of the NOP1 enhancer, and that repressing elements in toto are necessary to restrict the activity of the NOP1 enhancer in the nasal and otic placodes.

As the enhancer activity of the octameric 110–133 bp sequence was found to cover the entire neural plate and cephalic neural crest, in addition to the nasal and otic placodes, we expected that the TFs that bind to motifs 7 and 8 would also be expressed in these tissues. Sall4, a zinc-finger TF, was considered to be a strong candidate as a motif 7 binding factor for the following reasons: (1) the TAGAGC sequence of motif 7 resembles the known Sall4 binding sequence (Cho et al., 2008); (2) the expression of Sall4 shows a broad specificity similar to the activity of 110–133 bp octamer and is enhanced in the nasal and otic placode areas (Fig. 3D) as reported by Barembaum and Bronner-Fraser (2010); and (3) Sall4 has been shown to be essential for otic placode development (Barembaum and Bronner-Fraser, 2007). In contrast, none of the single Sox factors shows an expression pattern that could account for the enhancer activity of the 110–133 bp octamer. However, the combination of a few different Sox factors can have such tissue coverage. *SoxB1* genes, *Sox2* and *Sox3* genes, are expressed in the CNS and sensory placodes, but not in the neural crest at st. 11. On the other hand, *SoxE* genes, *Sox8*, *Sox9* and *Sox10*, are expressed in the cephalic neural crest, in addition to the nasal and otic placodes (Fig. 3D) (Betancur et al., 2011). These considerations raised the possibility that SoxB1 and SoxE factors cooperate with Sall4 in NOP1 enhancer activation through the elements located in the 110–133 bp fragment.

3.5. SoxB1/E factors and Sall4 synergistically activate the NOP1 110–133 enhancer

To test the hypothesis that SoxB1/E factors together with Sall4 activate the enhancer of the NOP1 110–133 bp fragment, we performed a series of reporter assays. A luciferase vector carrying an octameric 110–133 bp sequence was transfected into chick embryo fibroblasts, together with expression vectors for various TFs (Fig. 4A). Whilst the reporter vector harboring the 110–133 octamer showed minimal expression in these fibroblasts (Fig. 4Ba), an exogenous supply of Sox9 and Sall4 together, but not separately, strongly activated the 110–133 octamer as an enhancer (Fig. 4Bb). When the 110–133 bp sequence was mutated in either motif 7 or motif 8, the exogenous Sox9 and Sall4 combination failed to activate the enhancer (Fig. 4Bc, d). These observations indicated that the octamer of the 110–133 bp sequence of NOP1 is synergistically activated by Sox9 and Sall4 binding to motifs 8 and 7, respectively, and then operates as an enhancer. Using QT-6 quail fibroblast line, the NOP1 110–133 bp sequence was similarly activated by the combination of Sox8 and Sall4 (data not shown). The synergistic activation (> 10 fold) of the NOP1 110–133 bp sequence was also observed using Sox2 and Sox3 (SoxB1), but using Sox11 (a SoxC protein) Sall4-dependent activation was marginal (< 3 fold) (Fig. 4C). These results indicated that SoxB1/E factors in combination with Sall4 can activate the 110–133 bp sequence of NOP1 and that this is presumably a central process in the activation of full-length NOP1 enhancer in the nasal and otic placodes.

3.6. Inhibition of the NOP1 enhancer by repressor forms of a Sox TF

To confirm an essential function of Sox factors in the activation of the NOP1 enhancer in vivo, we expressed repressor forms of a Sox protein, Sox2-EnR, in the cephalic ectoderm of an electroporated chicken embryo, and examined their effects on NOP1 enhancer activity (Fig. 5A). As the DNA binding sequence is largely shared by all Sox TFs (Kamachi and Kondoh, 2013), Sox2-EnR was expected to interfere with the action of all SoxB1/SoxE TFs that activate the NOP1 enhancer

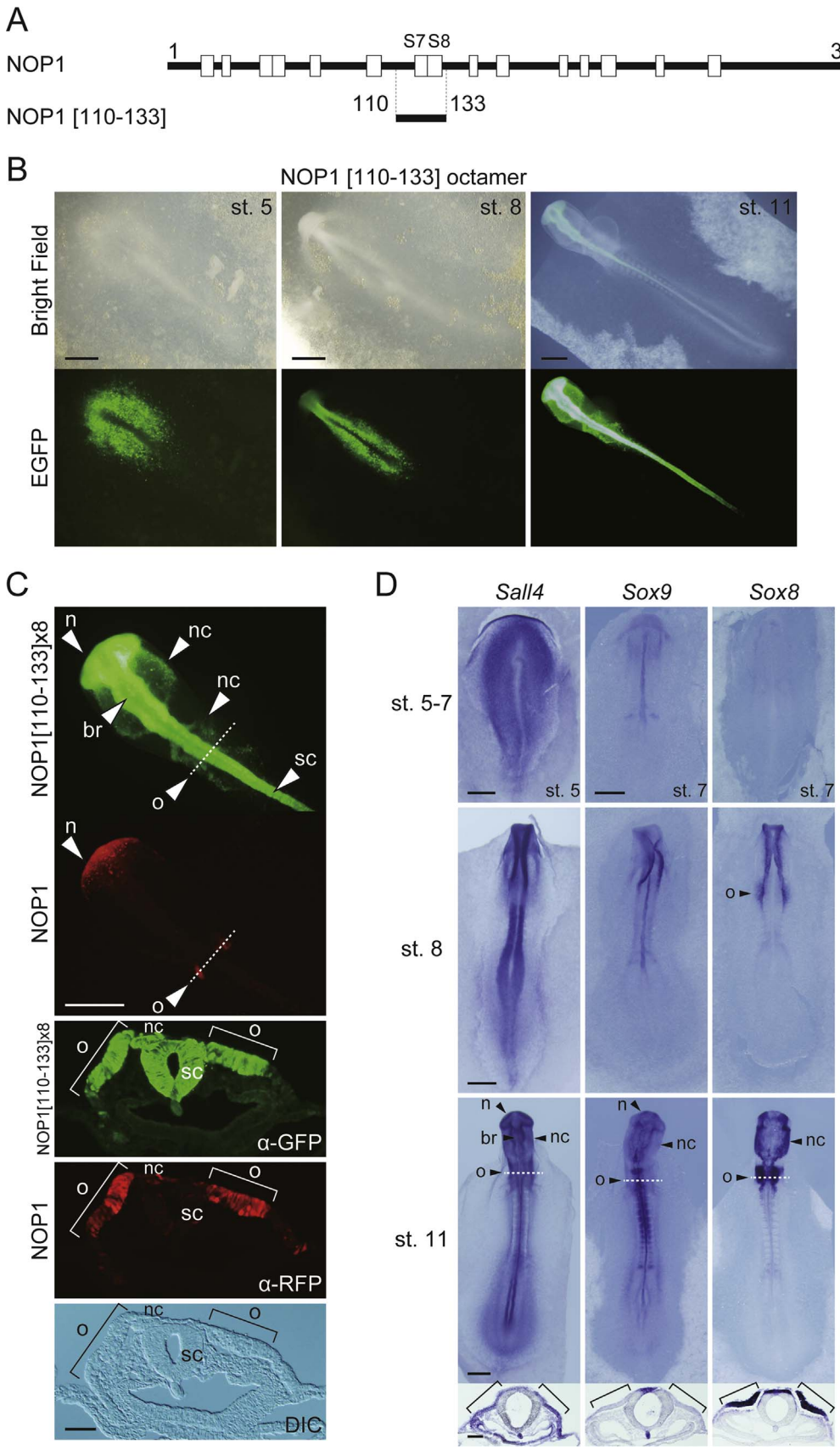

Fig. 3. Enhancer activity of the octamerized 110–133 bp sequence of NOP1 in ovo. (A) Schematic representation of the 110–133 bp sequence of NOP1, including motifs 7 and 8. (B) Enhancer activity of the octamerized 110–133 bp sequence in electroporated chicken embryos at st. 5, st. 8 (ventral images) and st. 11 (dorsal image). (C) Activity of the octamerized 110–133 bp sequence indicated by EGFP expression in comparison with full-length NOP1 enhancer activation of mRFP1 in the same embryo. A histological section across the otic placodes (along the broken line) was stained for GFP and RFP immunofluorescence, which indicated enhancer activities of NOP1 110–133 octamer and full length NOP1, respectively. Note that these enhancer activities overlap in the otic placodes. (D) Expression of *Sall4*, and group E *Sox9* and *Sox8* in chicken embryos at st. 5–7, 8 and 11 detected by in situ hybridization. Transverse sections through the otic placodes (along the broken line) were also shown in st. 11 embryos. Scale bars, 500 μm; 50 μm in section panels. Abbreviation: br, brain; nc, neural crest; n, nasal placode; o, otic placode; sc, spinal cord.

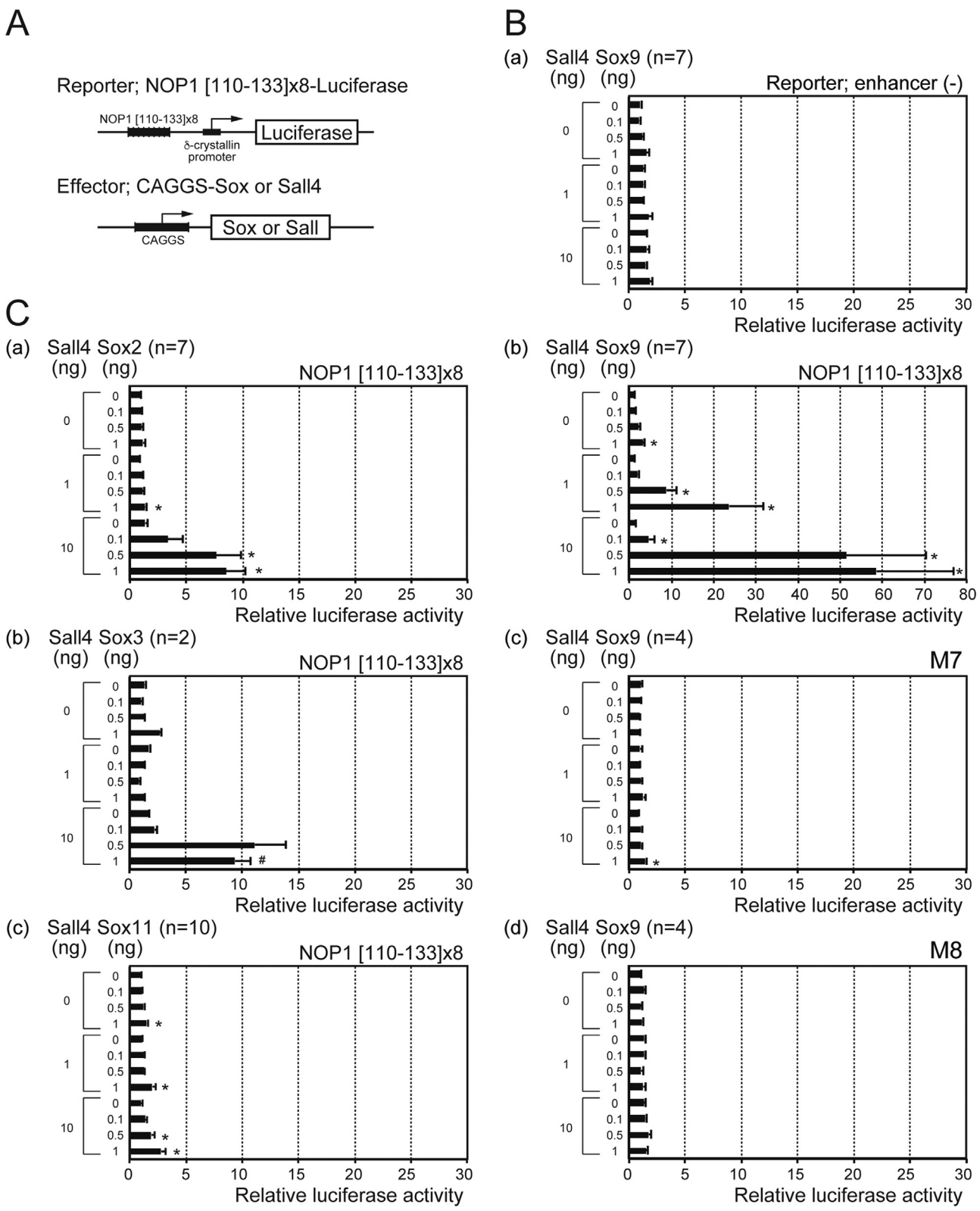

Fig. 4. Activation of the octamerized 110–133 bp sequence of NOP1 by the combined action of Sall4 and Sox factors. (A) Schematic representation of the luciferase reporter and effector vectors used in the experiments. (B) Activation with a combination of Sox9 and Sall4 of (a) an enhancer-less reporter; (b) an octamerized 110–133 bp sequence; and (c) and (d) an octamerized 110–133 bp sequence with M7 (c) or M8 (d) mutations that disrupt the Sall4 site (motif 7) or Sox site (motif 8). (C) (a) and (b). Activation of the reporter with octamerized 110–133 bp sequence using a combination of Sox2/3 and Sall4. (c) A marginal level of activation of the reporter by Sox11 and Sall4. The luciferase activity generated by the reporter without addition of effector plasmids was taken as 1. The number of biological replicates used to produce each bar graph is indicated in parentheses. The Student's two-tailed *t*-test was used to evaluate p-values between with and without a given level of Sox effector plasmid under the same Sall4 effector input. For the result indicated by #, the p value was 0.055. For other cases, the results with $p < 0.05$ are indicated by an asterisk.

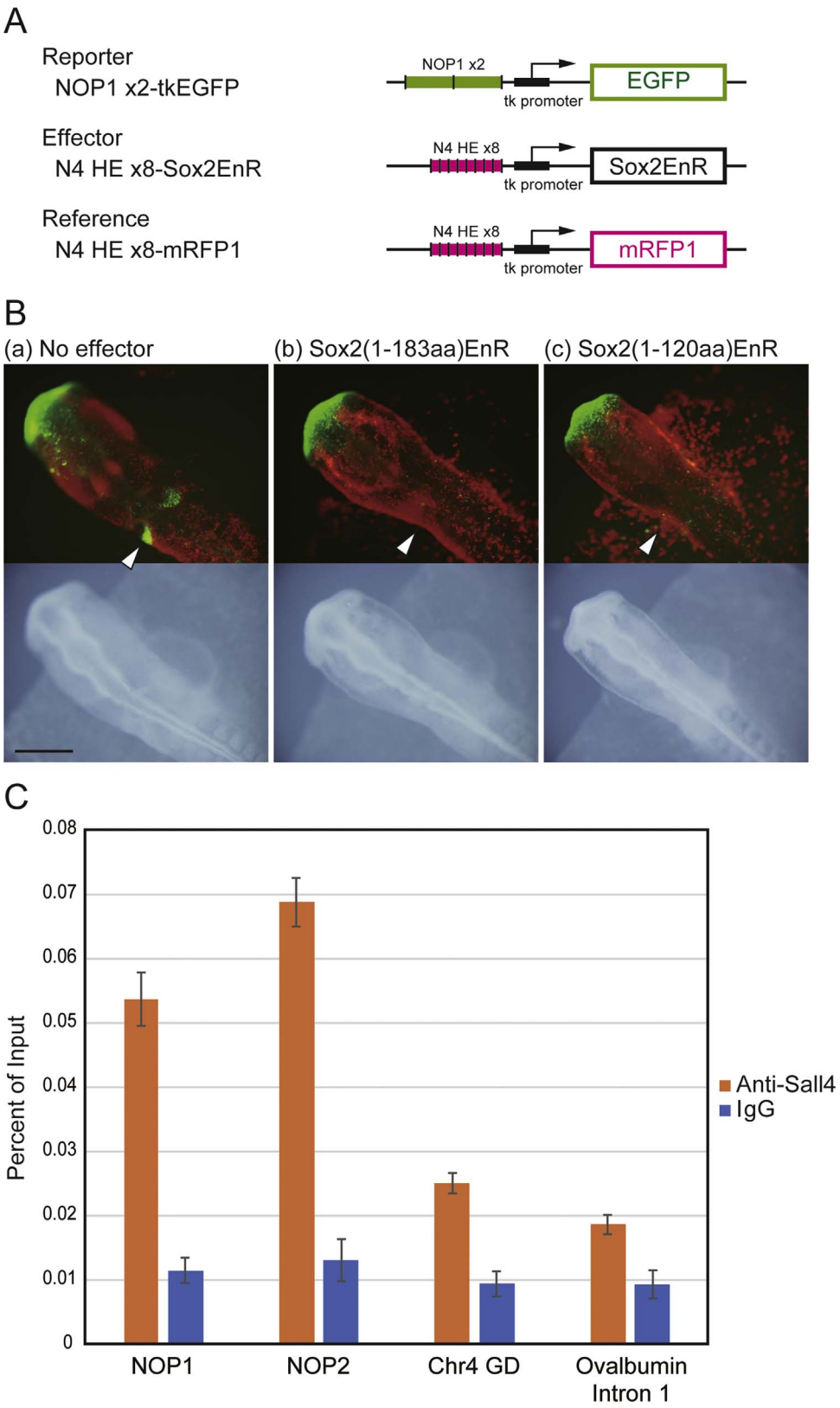

Fig. 5. Interaction of Sox and Sall4 TFs with the NOP1 sequence. (A) and (B) Effects of the inhibition of Sox activity by the posterior cephalic ectoderm-restricted expression of Sox2-EnR. (A) Schematic representation of the co-electroporated vectors used in the experiments. The octamerized N4HE enhancer was utilized to express exogenous genes restricted to the posterior cephalic ectoderm in an electroporated chicken embryo. (B) (a) Activities of NOP1 activating EGFP co-electroporated with octameric N4HE-mRFP1 showing the specificity of N4HE. (b) and (c) NOP1-EGFP co-electroporated with N4HE-Sox2-EnR and N4HE-mRFP1. The NOP1 enhancer activity in the otic placodes was lost following the expression of Sox2(1-183aa)-EnR (b) or Sox2(1-120aa)-EnR (c). Scale bar, 500 μm. (C) ChIP-qPCR analysis demonstrating preferential binding of Sall4 to NOP1 and NOP2 sequences in comparison with a sequence in chromosome 4 gene desert region (Chr4 GD) and ovalbumin gene intron 1 sequence. The averaged recovery of input sequences in percent, using anti-Sall4 and non-specific IgGs are presented. ChIP-qPCR with anti-Sall4 was performed using four biological replicates for each genomic site, whereas that with normal rabbit IgG was performed using three biological replicates. The Student's two-tailed *t*-tests was used for any pair of data sets, wherein significant differences were always indicated by $p < 0.05$. We particularly found that on comparing any pair of data sets between Sall4-binding sites (NOP1 and NOP2) and non-binding sites (Chr4 GD and Ovalbumin Intron 1), $p < 0.001$ was obtained, confirming that Sall4 binds to NOP1/NOP2 enhancer sequences.

together with Sall4. A cephalic ectoderm specific enhancer N4HE octamer was used to express Sox2-EnR constructs (Fig. 5A) (Saigou et al., 2010). The activity of N4HE octamer enhancer covers the otic placode, but not the nasal placode, allowing the use of the nasal placode as the control for unaffected placodal tissue. Two forms of Sox2-EnR fusion proteins, Sox2(183)EnR and Sox2(120)EnR, gave rise to identical results (Fig. 5B). When Sox2-EnR was expressed in the cephalic ectoderm, in the region demarcated by N4HE octamer-mRFP1 expression, NOP1-EGFP expression was totally lost from the otic placode region, whilst nasal placodal NOP1 activity, without receiving Sox2-EnR expression, remained unaffected (Fig. 5B). This result confirmed binding of Sox TFs to the NOP1 sequence.

3.7. ChIP-qPCR analysis of cephalic tissues in st. 11–12 chicken embryos, confirming binding of Sall4 to NOP1 and NOP2 sequences

To confirm binding of Sall4 to the Sox-Sall4 binding motif sequences of NOP1 and NOP2 enhancers, we performed ChIP-qPCR analysis of cephalic tissues from st. 11–12 chicken embryos anterior to the fourth somite level. A sequence in chromosome 4 gene desert region (Chr4 GD, the control sequence used by Murko and Bronner (2017)) and an ovalbumin intron 1 sequence were used as non-binding controls. As shown in Fig. 5C, ChIP using anti-Sall4 resulted significantly higher enrichment of NOP1 and NOP2 sequences compared to the Chr4 GD and ovalbumin intron 1 sequences, confirming specific binding of Sall4 to the enhancer regions.

3.8. Repression of the NOP1 enhancer activity by δEF1 (Zeb1) and Snail2 (Slug)

The multimeric form of the activation elements, the 110–133 bp sequence, and de-repressive NOP1 enhancer, NOP1 del-11, showed similar enhancer activity in the entire CNS and neural crest, in addition to the nasal and otic placodes (Fig. 3C, Suppl. Fig. 1A); this was because of the lack of major repressive elements. Mutations in sequence motifs 5 and 15, which share CACCT, strongly augmented the enhancer activity in the CNS and other cephalic tissues (Fig. 2C). CACCT is the canonical binding sequence of the repressor TFs δEF1 (Zeb1) and Sip1 (Zeb2), which are expressed in the CNS and neural crest but are absent from the nasal and otic placodes (Funahashi et al., 1993; Yasumi et al., 2016). The E2-box sequence CACCTG (motif 15) is the consensus binding sequence of Snail1 and Snail2 repressor TFs, and Snail2 is expressed in the chicken neural crest cells (Del Barrio and Nieto, 2004). These findings suggested that δEF1 and Snail2 repress the NOP1 enhancer activity in tissues outside the nasal and otic placodes, thereby producing placode specificity of the enhancer. To test this model, two approaches were taken to ectopically express above-mentioned repressor TFs in the embryonic ectoderm that covers the otic placode region, in order to see if the NOP1 activity in the otic placode region is repressed. First, NOP1-tkEGFP and δEF1/Snail2 expression vectors driven by the N4HE octamer enhancer (Saigou et al., 2010) were coelectroporated in st. 4 embryos. The NOP1-dependent EGFP expression in the otic placodes was totally inhibited, whereas that in the nasal placode remained active (Fig. 6A). Second, NOP1-tkEGFP was electroporated at st. 4 over the entire epiblast and then expression vectors for δEF1 or Snail2 plus mRFP1 were ectopically expressed at st. 7 on one side of the cephalic ectoderm of the embryo, which included the otic placode area (Fig. 6B). Expression of δEF1 completely repressed the enhancer activity on the otic placode of electroporated side marked by the mRFP1 expression. These results demonstrated that δEF1 and Snail2 can repress the NOP1 enhancer when they are expressed, and support the model that repression by δEF1 or Snail2 contributes to the placode specificity of the NOP1 enhancer.

3.9. The transcription factor gene activation order leading to Sox2 activation in the otic placode

The above results indicated that Sox2, Sox3, Sox8, and Sox9, in combination with Sall4 can activate the NOP1 enhancer. To determine the sequence of activation of these TF genes leading to *Sox2* activation in the otic placode, we investigated the expression of these genes in the otic placode region following the developmental stages using in situ hybridization (Fig. 7A). Whereas *Sall4* was expressed from before otic placode development, *Sox3* and *Sox8* were activated at st. 8 in the otic placode precursor area, prior to *Sox2* and *Sox9* activation at st. 10. It is therefore possible that Sox3 and Sox8 together with Sall4 initiate *Sox2* expression via the NOP1/2 enhancers in the otic placode. After st. 10, Sox9 may also participate in the NOP1/2 enhancer activation. Once the *Sox2* gene is activated, it is possible that Sox2 in combination with Sall4 sustain *Sox2* expression in the later development of otic placode derivatives via NOP1/2 as an auto-activation loop (Fig. 7B).

4. Discussion

4.1. Combination of activation and repression mechanisms in the regulation of the NOP1 enhancer

In many enhancer analyses conducted previously, the primary focus was on the interaction of activating TFs with the enhancer sequence, with the basic idea that the activating factor is a primary determinant of enhancer specificity. In our study, however, we describe a system in which repressive mechanisms determine tissue specificity of an enhancer. Deletion and mutational analyses conducted in this study indicate that the NOP1 enhancer sequence is composed of multiple activating and repressing elements (Fig. 2). Major elements highlighted in this study are the 110–133 bp region containing activating motifs 7 and 8. Deletion and mutational analyses of the NOP1 sequence also identified auxiliary activating elements and multiple repressing elements, the latter exemplified by motifs 2, 5, 6, 9 and 15. Mutation of these repressing elements not only augmented the NOP1 enhancer activity, but also widened enhancer-active regions in the cephalic tissues. These observations indicate that delimitation of the NOP1 enhancer specificity to the nasal and otic placodes primarily depends on repressive mechanisms, suggesting that the nasal and otic placodes are formed in the embryonic regions where such repressing mechanisms are weak enough to be overcome by activation mechanisms.

4.2. Sall4 as a partner factor of SoxB1 and SoxE in the activation of the NOP1 enhancer

Sall4 has been found to be involved in inner ear development as a haploinsufficiency of this TF is causative for Okihiro syndrome associated with deafness in human patients and in knockout mice (Borozdin et al., 2004; Kohlhase et al., 2002; Warren et al., 2007). Sox9 and Sox2 are coexpressed in the otic placode to otocyst (Mak et al., 2009), *Sall4* or *Sox9* defects interfere with otic placode invagination (Barembaum and Bronner-Fraser, 2007; Barrionuevo et al., 2008). In addition, the otic placode-specific enhancer for Sall4 has also been identified (Barembaum and Bronner-Fraser, 2010). The *Sox8* expression pattern in the CNS and cephalic neural crest at st. 11 resembles the tissue distribution of non-placodal enhancer activities found using repressive element-inactivated NOP1 mutants and the activity of octameric 110–133 enhancer devoid of repressing elements (Fig. 3B–D, Suppl. Fig. 1). This observation suggested the contribution of Sox8 largely in the cryptic non-placodal enhancer activity of NOP1. Mutant mice with an inner ear-specific defect of *Sox2* expression (*Llc* and *Ysb*) lack the sensory and neural primordia of the inner ear (Kiernan et al., 2005). In this study, we demonstrate that the action of these TFs converges in the NOP1 enhancer regulation, revealing an important intersection point of multiple regulatory pathways during inner ear development.

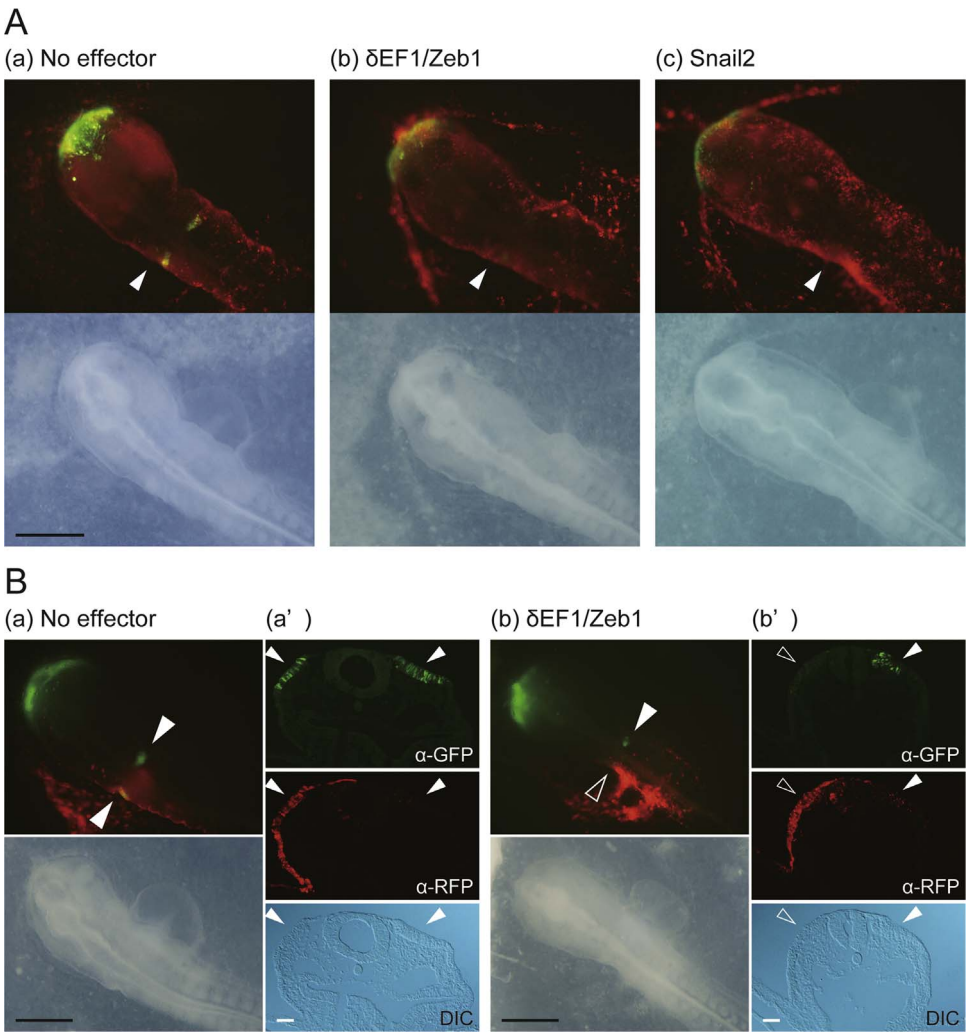

Fig. 6. Repression of the NOP1 enhancer activity by δEF1/Zeb1 and Snail2. (A) NOP1-tkEGFP, N4HE-δEF1/Zeb1 or Snail2, and N4HE-mRFP1 were co-electroporated in st. 4 chicken embryo and examined at st. 11. The NOP1 enhancer activity in the otic placodes was lost following the expression of N4HE-δEF1/Zeb1 (b) or N4HE-Snail2 (c). (B) Sequential electroporation of the NOP1-ptkEGFP and pCAGGS-δEF1/Zeb1. NOP1-tkEGFP was electroporated at st. 4, followed by a second electroporation at. st. 7 in one side of the epiblast with pCAGGS-δEF1/Zeb1 and pCMV-mRFP1, the latter marking the electroporated tissues. (a) Expression of EGFP activated by NOP1; (b) EGFP expression after expression of δEF1/Zeb1 at st. 7. The NOP1 enhancer activity in the otic placode was repressed by the expression of δEF1/Zeb1. (a′) and (b′) represent the histological sections across otic placodes (arrowheads) of specimens (a) and (b) stained for EGFP and mRFP1 immunofluorescence or processed for DIC images. Scale bar, 500 μm; 50 μm in section panels.

The combination of motifs 7 and 8 represent binding sites for Sall4 and Sox proteins, and these sites are essential for NOP1 enhancer activity as mutations of either site diminishes this activity (Fig. 2C). The octamerized 110–133 bp region were activated by the combination of Sall4 and Sox2/3 (SoxB1), or Sall4 and Sox9 (SoxE) in our reporter assays (Fig. 4). The requirement of Sox functions for NOP1 activation was also demonstrated by the effects of a dominant-negative form of Sox TFs (Sox2-EnR), which totally inhibited NOP1 activity in the chicken embryo (Fig. 5B). NOP2 enhancer also possesses an analogous Sox-Sall4 co-binding sequence, and ChIP-qPCR analyses demonstrated binding of Sall4 to the NOP1 and NOP2 enhancer sequences in vivo (Fig. 5C). Timings of activation of NOP1 and NOP2 are similar (Uchikawa et al., 2003). It is likely that NOP1 and NOP2 have redundant functions, as in mouse NOP2 lacks the enhancer activity possibly due to multiple mutations (Suppl. Fig. 2). NOP1 sequence is strongly conserved in vertebrate species from amphibians to mammals, suggesting that Sox-Sall4 dependent regulation of naso-otic placode development is conserved across these species.

4.3. Initiation vs maintenance mechanisms of NOP1 activation

In the nasal and otic placode precursors, *Sox3* and *Sox8* are the earliest to be expressed at st. 8 among the *SoxB1/E* genes (Fig. 7A) (Rex et al., 1997; Uchikawa et al., 2011). A possible model shown in Fig. 7B is that Sox3/8 first interact with Sall4 and activate *Sox2* expression in the otic placode via NOP1/2 enhancers around st. 10. After st. 10, Sox9 is also activated in the otic placode, and possibly contributes to NOP1/2 activation. Then, Sox2 together with Sall4 maintains *Sox2* expression in the otic placode even at later stages of the inner ear development (Evsen et al., 2013; Neves et al., 2012). The involvement of the Sox2 autoregulatory loop in cooperation with a partner factor has precedence in lens placode development, where *Sox2* expression induced by the activation of the N3 enhancer is sustained by an autoregulatory loop aided by partner factor Pax6 (Inoue et al., 2007; Kamachi and Kondoh, 2013).

4.4. Possible involvement of Wnt and Fgf signaling in the activation of the NOP1 enhancer

Our analysis indicated that mutations in motifs 4 and 10 also strongly inactivated the NOP1 enhancer (Fig. 2, Suppl. Fig. 1B). These motifs account for activation elements in the 41–60 and 154–173 bp regions, respectively, as predicted by our deletion analysis. Motif 4 is similar to the Fgf-response sequence TGTGAC previously reported for the N1 enhancer (Takemoto et al., 2006). Motif 10 conforms to the Lef/

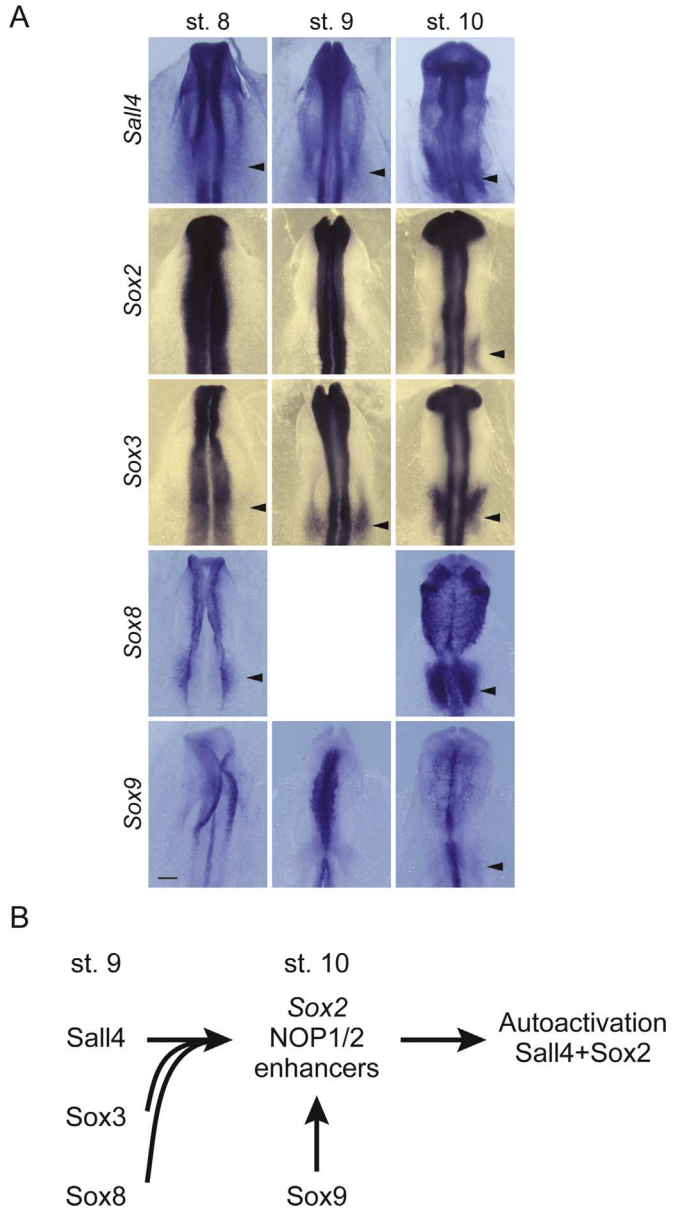

Fig. 7. Sequential activation of Sox TF genes involved in the NOP1 enhancer regulation in the otic placode. (A) Expression of *Sall4*, *Sox2*, *Sox3*, *Sox8* and *Sox9* in the embryos at st. 8, 9, and 10 is shown by in situ hybridization. The arrowheads indicate their expression in otic placode or its precursors. Scale bar, 200 μm. While *Sall4* expression in the otic placode precursors starts earlier than these stages, expression of *Sox3* and *Sox8* initiates at st. 8, and that of *Sox2* and *Sox9* initiates at st. 10. Although *Sox8* expression data at st. 9 is not available, we presume that *Sox8* expression is kept on at this stage. (B) A model of two steps of NOP1/2 enhancer activation based on above observations. Around st. 9 when Sox3 and Sox8 expression levels will become high enough, these Sox TFs together with Sall4 bind to the adjacent DNA sites of the NOP1/2 enhancers, leading to *Sox2* activation around st. 10. Sox9 may join activation of NOP1/2 at this stage. Once *Sox2* expression is activated in the otic placode, Sox2 cooperates with Sall4 to maintain *Sox2* expression to later developmental stages of inner ear development via NOP1/2-dependent autoactivation.

Tcf-binding sequence, [T/A][T/A]CAAA (Giese et al., 1991), raising the possibility that the Fgf and canonical Wnt/β-catenin signaling pathways regulate gene expression of *Sox2* during nasal and otic development, which is consistent with the documented Wnt and Fgf signal inputs to the early stages of inner ear development (Ohyama et al., 2007). It is interesting to note that the putative Wnt- and Fgf-responsive elements are also found in the NOP2 enhancer sequence (Suppl. Fig. 2).

4.5. Repression of the NOP1 enhancer outside the sensory tissues by CACCT/CACCTG-binding proteins

The del-9 to del-11 mutant enhancers and the octameric 110–133 sequence, including motifs 7 and 8, were found to be strongly activated in the CNS and cephalic neural crest without being limited to the nasal and otic placodes. This indicated that the activating elements by themselves do not determine the specificity of this enhancer, but the repressive elements primarily determine the NOP1 enhancer specificity. Mutational analysis registered motifs 2, 5, 6, 9 and 15 as repressive elements (Fig. 2A(b)).

Motif 5 consists of CACCT, the binding site of Zeb family TFs δEF1 (Zeb1) and Sip1 (Zeb2) (Sekido et al., 1997; Verschueren et al., 1999), and motif 15 consists of CACCTG (E2 box sequence) that serves as the binding site for Zeb family TFs and Snail family TFs Snail1 and Snail2 (Batlle et al., 2000; Cano et al., 2000). These TFs primarily act as repressors, even counteracting with E2 box-binding activator TFs (Batlle et al., 2000; Cano et al., 2000; Nieto, 2002; Sekido et al., 1994; van Grunsven et al., 2001; Verschueren et al., 1999).

It is also interesting to note that δEF1, Sip1 and Snail2 are expressed in the cephalic tissues of chicken embryos in such a way as to circumvent the forming otic vesicle or nasal pit (Funahashi et al., 1993; Sefton et al., 1998; Yasumi et al., 2016), whereas Snail1 is not expressed in the cephalic tissues in chicken embryos. Therefore, it is likely that δEF1 and Sip1 that interact with motif 5, and δEF1, Sip1 and Snail2 that interact with motif 15 repress the NOP1 enhancer activity in the tissues where they are expressed. To test this model, we investigated whether overexpression of δEF1 or Snail2 in the otic placode area represses the NOP1 enhancer activity in the otic placode/vesicle. We demonstrated the repressive activities of these TFs in the experiments shown in Fig. 6. Exogenous expression of δEF1 or Snail2 in the cephalic ectodermal areas that covers the otic placode/vesicle region or one side of the ectoderm totally repressed NOP1 activity in the relevant embryonic regions. We can, therefore, conclude that δEF1, and probably Sip1, repress NOP1 enhancer activity via motif 5, whereas δEF1, Sip1 and Snail2 do so via motif 15, and these repressions contribute to delimiting NOP1 enhancer activity to the nasal and otic placodes. The subtle differences in the effect of the mutations in motifs 5 and 15, may reflect the difference in the participating repressors; motif 5 mutation primarily derepressed the NOP1 enhancer activity in the CNS, whereas motif 15 did so in a wider spectrum of tissues (Fig. 2C).

Motif 15 represents the E2 box sequence where bHLH TFs also interact. This motif has been shown to act as a binding site for repressive bHLH factor Neurod1 and is essential for downregulating *Sox2* during the maturation stage of neural development in the inner ear (Evsen et al., 2013). Therefore, this motif in the NOP1 enhancer is very important for *Sox2* regulation in the context of inner ear development.

4.6. Implications from the NOP1 enhancer regulation concerning the process of placodal specification

The earlier studies on the progressive specification of the PPR indicated major contributions of antero-posterior differences in the signal inputs and region-specific activating TFs, resulting in the emphasis of the association of nasal-lens placodes and otic-epibranchial placodes (Lleras-Forero and Streit, 2012; Schlosser and Ahrens, 2004; Streit, 2004). However, there are also commonalities between the nasal and otic placode development (Streit, 2004), as indicated by dependence on specific TFs, such as Dlx5 (Depew et al., 1999) and Foxg1 (Duggan et al., 2008; Pauley et al., 2006). This study has revealed an additional link between the nasal and otic placode development that is commonly dependent on Sox-Sall4 interaction and distinguishes them from other placodes. These observations indicate the operation of very complex regulatory interactions during the specification of sensory placodes.

We also identified nasal and otic monospecific enhancers that are located at distant positions from the *Sox2* gene (Okamoto et al., 2015; Uchikawa and Kondoh, 2016) or are associated with the *Sox3* gene (Nishimura et al., 2012). Comparison of these enhancers with the NOP1 enhancer may reveal steps in the progressive specification of the nasal and otic placodes in the context of *Sox2* regulation.

Acknowledgements

We thank Doris Wu and the members of Kondoh lab for helpful and stimulating discussions. We also thank Tatsuya Tanaka at Center for Medical Research and Education, Graduate School of Medicine, Osaka University for his technical assistance. This study was supported by a grant from the Takeda Science Foundation to HK and Grants-in-Aid for Scientific Research JP22247035, JP26251024 and JP17H03680 to HK and JP23770248, JP25440106 and JP16K07370 to MU from MEXT Japan.

Appendix A. Supporting information

Supplementary data associated with this article can be found in the online version at doi:10.1016/j.ydbio.2017.11.005.

References

Ahmed, M., Wong, E.Y., Sun, J., Xu, J., Wang, F., Xu, P.X., 2012. Eya1-Six1 interaction is sufficient to induce hair cell fate in the cochlea by activating Atoh1 expression in cooperation with Sox2. Dev. Cell 22, 377–390.
Baker, C.V., Bronner-Fraser, M., 2001. Vertebrate cranial placodes I. Embryonic induction. Dev. Biol. 232, 1–61.
Barembaum, M., Bronner-Fraser, M., 2007. Spalt4 mediates invagination and otic placode gene expression in cranial ectoderm. Development 134, 3805–3814.
Barembaum, M., Bronner-Fraser, M., 2010. Pax2 and Pea3 synergize to activate a novel regulatory enhancer for spalt4 in the developing ear. Dev. Biol. 340, 222–231.
Barrionuevo, F., Naumann, A., Bagheri-Fam, S., Speth, V., Taketo, M.M., Scherer, G., Neubuser, A., 2008. Sox9 is required for invagination of the otic placode in mice. Dev. Biol. 317, 213–224.
Batlle, E., Sancho, E., Franci, C., Dominguez, D., Monfar, M., Baulida, J., Garcia De Herreros, A., 2000. The transcription factor snail is a repressor of E-cadherin gene expression in epithelial tumour cells. Nat. Cell Biol. 2, 84–89.
Betancur, P., Sauka-Spengler, T., Bronner, M., 2011. A Sox10 enhancer element common to the otic placode and neural crest is activated by tissue-specific paralogs. Development 138, 3689–3698.
Bhattacharyya, S., Bronner-Fraser, M., 2008. Competence, specification and commitment to an olfactory placode fate. Development 135, 4165–4177.
Borozdin, W., Boehm, D., Leipoldt, M., Wilhelm, C., Reardon, W., Clayton-Smith, J., Becker, K., Muhlendyck, H., Winter, R., Giray, O., Silan, F., Kohlhase, J., 2004. SALL4 deletions are a common cause of Okihiro and acro-renal-ocular syndromes and confirm haploinsufficiency as the pathogenic mechanism. J. Med. Genet. 41, e113.
Cano, A., Perez-Moreno, M.A., Rodrigo, I., Locascio, A., Blanco, M.J., del Barrio, M.G., Portillo, F., Nieto, M.A., 2000. The transcription factor snail controls epithelial-mesenchymal transitions by repressing E-cadherin expression. Nat. Cell Biol. 2, 76–83.
Cho, S.Y., Chung, M., Park, M., Park, S., Lee, Y.S., 2008. ZIFIBI: prediction of DNA binding sites for zinc finger proteins. Biochem. Biophys. Res. Commun. 369, 845–848.
Del Barrio, M.G., Nieto, M.A., 2004. Relative expression of Slug, RhoB, and HNK-1 in the cranial neural crest of the early chicken embryo. Dev. Dyn. 229, 136–139.
Depew, M.J., Liu, J.K., Long, J.E., Presley, R., Meneses, J.J., Pedersen, R.A., Rubenstein, J.L., 1999. Dlx5 regulates regional development of the branchial arches and sensory capsules. Development 126, 3831–3846.
Duggan, C.D., DeMaria, S., Baudhuin, A., Stafford, D., Ngai, J., 2008. Foxg1 is required for development of the vertebrate olfactory system. J. Neurosci. 28, 5229–5239.
Evsen, L., Sugahara, S., Uchikawa, M., Kondoh, H., Wu, D.K., 2013. Progression of neurogenesis in the inner ear requires inhibition of Sox2 transcription by neurogenin1 and neurod1. J. Neurosci. 33, 3879–3890.
Funahashi, J., Sekido, R., Murai, K., Kamachi, Y., Kondoh, H., 1993. Delta-crystallin enhancer binding protein deltaEF1 is a zinc finger-homeodomain protein implicated in postgastrulation embryogenesis. Development 119, 433–446.
Giese, K., Amsterdam, A., Grosschedl, R., 1991. DNA-binding properties of the HMG domain of the lymphoid-specific transcriptional regulator LEF-1. Genes Dev. 5, 2567–2578.
Goto, K., Okada, T.S., Kondoh, H., 1990. Functional cooperation of lens-specific and nonspecific elements in the delta 1-crystallin enhancer. Mol. Cell Biol. 10, 958–964.
Groves, A.K., Bronner-Fraser, M., 2000. Competence, specification and commitment in otic placode induction. Development 127, 3489–3499.
Hamburger, V., Hamilton, H.L., 1951. A series of normal stages in the development of the chick embryo. J. Morph. 88, 49–92.
Hatakeyama, J., Shimamura, K., 2008. Method for electroporation for the early chick embryo. Dev. Growth Differ. 50, 449–452.
Inoue, M., Kamachi, Y., Matsunami, H., Imada, K., Uchikawa, M., Kondoh, H., 2007. PAX6 and SOX2-dependent regulation of the Sox2 enhancer N-3 involved in embryonic visual system development. Genes Cells 12, 1049–1061.
Jacobson, A.G., 1963. The determination and positioning of the nose, lens and ear. III. Effects of reversing the antero-posterior axis of epidermis, neural plate and neural fold. J. Exp. Zool. 154, 293–303.
Jolma, A., Yan, J., Whitington, T., Toivonen, J., Nitta, K.R., Rastas, P., Morgunova, E., Enge, M., Taipale, M., Wei, G., Palin, K., Vaquerizas, J.M., Vincentelli, R., Luscombe, N.M., Hughes, T.R., Lemaire, P., Ukkonen, E., Kivioja, T., Taipale, J., 2013. DNA-binding specificities of human transcription factors. Cell 152, 327–339.
Kamachi, Y., Kondoh, H., 1993. Overlapping positive and negative regulatory elements determine lens-specific activity of the delta 1-crystallin enhancer. Mol. Cell Biol. 13, 5206–5215.
Kamachi, Y., Kondoh, H., 2013. Sox proteins: regulators of cell fate specification and differentiation. Development 140, 4129–4144.
Kamachi, Y., Uchikawa, M., Collignon, J., Lovell-Badge, R., Kondoh, H., 1998. Involvement of Sox1, 2 and 3 in the early and subsequent molecular events of lens induction. Development 125, 2521–2532.
Kamachi, Y., Uchikawa, M., Kondoh, H., 2000. Pairing SOX off: with partners in the regulation of embryonic development. Trends Genet. 16, 182–187.
Kamachi, Y., Iwafuchi, M., Okuda, Y., Takemoto, T., Uchikawa, M., Kondoh, H., 2009. Evolution of non-coding regulatory sequences involved in the developmental process: reflection of differential employment of paralogous genes as highlighted by Sox2 and group B1 Sox genes. Proc. Jpn. Acad. Ser. B Phys. Biol. Sci. 85, 55–68.
Kiernan, A.E., Pelling, A.L., Leung, K.K., Tang, A.S., Bell, D.M., Tease, C., Lovell-Badge, R., Steel, K.P., Cheah, K.S., 2005. Sox2 is required for sensory organ development in the mammalian inner ear. Nature 434, 1031–1035.
Ko, L.J., Engel, J.D., 1993. DNA-binding specificities of the GATA transcription factor family. Mol. Cell Biol. 13, 4011–4022.
Kohlhase, J., Heinrich, M., Schubert, L., Liebers, M., Kispert, A., Laccone, F., Turnpenny, P., Winter, R.M., Reardon, W., 2002. Okihiro syndrome is caused by SALL4 mutations. Hum. Mol. Genet. 11, 2979–2987.
Kondoh, H., Kamachi, Y., 2010. SOX-partner code for cell specification: regulatory target selection and underlying molecular mechanisms. Int. J. Biochem. Cell Biol. 42, 391–399.
Kondoh, H., Uchikawa, M., 2008. Chapter 17 Dissection of Chick Genomic Regulatory Regions. Methods Cell Biol. 87, 313–336.
Lleras-Forero, L., Streit, A., 2012. Development of the sensory nervous system in the vertebrate head: the importance of being on time. Curr. Opin. Genet. Dev. 22, 315–322.
Mak, A.C., Szeto, I.Y., Fritzsch, B., Cheah, K.S., 2009. Differential and overlapping expression pattern of SOX2 and SOX9 in inner ear development. Gene Expr. Patterns 9, 444–453.
Matsumata, M., Uchikawa, M., Kamachi, Y., Kondoh, H., 2005. Multiple N-cadherin enhancers identified by systematic functional screening indicate its Group B1 SOX-dependent regulation in neural and placodal development. Dev. Biol. 286, 601–617.
Murko, C., Bronner, M.E., 2017. Tissue specific regulation of the chick Sox10E1 enhancer by different Sox family members. Dev. Biol. 422, 47–57.
Neves, J., Parada, C., Chamizo, M., Giraldez, F., 2011. Jagged 1 regulates the restriction of Sox2 expression in the developing chicken inner ear: a mechanism for sensory organ specification. Development 138, 735–744.
Neves, J., Uchikawa, M., Bigas, A., Giraldez, F., 2012. The prosensory function of Sox2 in the chicken inner ear relies on the direct regulation of Atoh1. PLoS One 7, e30871.
Nieto, M.A., 2002. The snail superfamily of zinc-finger transcription factors. Nat. Rev. Mol. Cell Biol. 3, 155–166.
Nishimura, N., Kamimura, Y., Ishida, Y., Takemoto, T., Kondoh, H., Uchikawa, M., 2012. A systematic survey and characterization of enhancers that regulate Sox3 in neuro-sensory development in comparison with Sox2 enhancers. Biology 1, 714–735.
Niwa, H., Yamamura, K., Miyazaki, J., 1991. Efficient selection for high-expression transfectants with a novel eukaryotic vector. Gene 108, 193–199.
Ohyama, T., Groves, A.K., Martin, K., 2007. The first steps towards hearing: mechanisms of otic placode induction. Int. J. Dev. Biol. 51, 463–472.
Okamoto, R., Uchikawa, M., Kondoh, H., 2015. Sixteen additional enhancers associated with the chicken Sox2 locus outside the central 50-kb region. Dev. Growth Differ. 57, 24–39.
Overdier, D.G., Ye, H., Peterson, R.S., Clevidence, D.E., Costa, R.H., 1997. The winged helix transcriptional activator HFH-3 is expressed in the distal tubules of embryonic and adult mouse kidney. J. Biol. Chem. 272, 13725–13730.
Pauley, S., Lai, E., Fritzsch, B., 2006. Foxg1 is required for morphogenesis and histogenesis of the mammalian inner ear. Dev. Dyn. 235, 2470–2482.
Rex, M., Orme, A., Uwanogho, D., Tointon, K., Wigmore, P.M., Sharpe, P.T., Scotting, P.J., 1997. Dynamic expression of chicken Sox2 and Sox3 genes in ectoderm induced to form neural tissue. Dev. Dyn. 209, 323–332.
Saigou, Y., Kamimura, Y., Inoue, M., Kondoh, H., Uchikawa, M., 2010. Regulation of Sox2 in the pre-placodal cephalic ectoderm and central nervous system by enhancer N-4. Dev. Growth Differ. 52, 397–408.
Schlosser, G., 2006. Induction and specification of cranial placodes. Dev. Biol. 294, 303–351.
Schlosser, G., Ahrens, K., 2004. Molecular anatomy of placode development in Xenopus laevis. Dev. Biol. 271, 439–466.
Sefton, M., Sanchez, S., Nieto, M.A., 1998. Conserved and divergent roles for members of the Snail family of transcription factors in the chick and mouse embryo. Development 125, 3111–3121.
Sekido, R., Murai, K., Funahashi, J., Kamachi, Y., Fujisawa-Sehara, A., Nabeshima, Y., Kondoh, H., 1994. The delta-crystallin enhancer-binding protein delta EF1 is a repressor of E2-box-mediated gene activation. Mol. Cell Biol. 14, 5692–5700.

Sekido, R., Murai, K., Kamachi, Y., Kondoh, H., 1997. Two mechanisms in the action of repressor deltaEF1: binding site competition with an activator and active repression. Genes Cells 2, 771–783.
Spitz, F., Demignon, J., Porteu, A., Kahn, A., Concordet, J.P., Daegelen, D., Maire, P., 1998. Expression of myogenin during embryogenesis is controlled by Six/sine oculis homeoproteins through a conserved MEF3 binding site. Proc. Natl. Acad. Sci. USA 95, 14220–14225.
Streit, A., 2004. Early development of the cranial sensory nervous system: from a common field to individual placodes. Dev. Biol. 276, 1–15.
Streit, A., 2007. The preplacodal region: an ectodermal domain with multipotential progenitors that contribute to sense organs and cranial sensory ganglia. Int. J. Dev. Biol. 51, 447–461.
Takemoto, T., Uchikawa, M., Kamachi, Y., Kondoh, H., 2006. Convergence of Wnt and FGF signals in the genesis of posterior neural plate through activation of the Sox2 enhancer N-1. Development 133, 297–306.
Tanaka, S., Kamachi, Y., Tanouchi, A., Hamada, H., Jing, N., Kondoh, H., 2004. Interplay of SOX and POU factors in regulation of the Nestin gene in neural primordial cells. Mol. Cell Biol. 24, 8834–8846.
Uchikawa, M., 2008. Enhancer analysis by chicken embryo electroporation with aid of genome comparison. Dev. Growth Differ. 50, 467–474.
Uchikawa, M., Kondoh, H., 2016. Regulation of Sox2 via many enhancers of distinct specificities. In: Kondoh, H., Lovell-Badge, R. (Eds.), Sox2: Biology and Role in Development an Disease. Academic Press/Elsevier, Boston, Oxford, San Diego, 107–129.
Uchikawa, M., Ishida, Y., Takemoto, T., Kamachi, Y., Kondoh, H., 2003. Functional analysis of chicken Sox2 enhancers highlights an array of diverse regulatory elements that are conserved in mammals. Dev. Cell 4, 509–519.
Uchikawa, M., Takemoto, T., Kamachi, Y., Kondoh, H., 2004. Efficient identification of regulatory sequences in the chicken genome by a powerful combination of embryo electroporation and genome comparison. Mech. Dev. 121, 1145–1158.
Uchikawa, M., Yoshida, M., Iwafuchi-Doi, M., Matsuda, K., Ishida, Y., Takemoto, T., Kondoh, H., 2011. B1 and B2 Sox gene expression during neural plate development in chicken and mouse embryos: universal versus species-dependent features. Dev. Growth Differ. 53, 761–771.
Uchikawa, M., Nishimura, N., Iwafuchi-Doi, M., Kondoh, H., 2017. Enhancer analyses using chicken embryo electroporation. Methods Mol. Biol. 1650, 191–202.
van Grunsven, L.A., Schellens, A., Huylebroeck, D., Verschueren, K., 2001. SIP1 (Smad interacting protein 1) and deltaEF1 (delta-crystallin enhancer binding factor) are structurally similar transcriptional repressors. J. Bone Jt. Surg. Am. 83-A (Suppl. 1), S40–S47.
Verschueren, K., Remacle, J.E., Collart, C., Kraft, H., Baker, B.S., Tylzanowski, P., Nelles, L., Wuytens, G., Su, M.T., Bodmer, R., Smith, J.C., Huylebroeck, D., 1999. SIP1, a novel zinc finger/homeodomain repressor, interacts with Smad proteins and binds to 5′-CACCT sequences in candidate target genes. J. Biol. Chem. 274, 20489–20498.
Warren, M., Wang, W., Spiden, S., Chen-Murchie, D., Tannahill, D., Steel, K.P., Bradley, A., 2007. A Sall4 mutant mouse model useful for studying the role of Sall4 in early embryonic development and organogenesis. Genesis 45, 51–58.
Yasumi, T., Inoue, M., Maruhashi, M., Kamachi, Y., Higashi, Y., Kondoh, H., Uchikawa, M., 2016. Regulation of trunk neural crest delamination by deltaEF1 and Sip1 in the chicken embryo. Dev. Growth Differ. 58, 205–214.
Zou, D., Erickson, C., Kim, E.H., Jin, D., Fritzsch, B., Xu, P.X., 2008. Eya1 gene dosage critically affects the development of sensory epithelia in the mammalian inner ear. Hum. Mol. Genet. 17, 3340–3356.